Cooperating Mobile Cable Robots: Screw Theoretic Analysis

Xiaobo Zhou, Chin Pei Tang, and Venkat Krovi

Abstract. Cable robots form a class of parallel architecture robots with significant benefits including simplicity of construction, large workspace, significant payload capacity and end effector stiffness. While conventional cable robots have fixed bases, we seek to explore inclusion of mobility into the bases (in the form of gantries, and/or vehicle bases) which can significantly further enhance the capabilities of cable robots. However, this also introduces redundancy and complexity into the system which needs to be carefully analyzed and resolved. To this end, we propose a generalized modeling framework for systematic design and analysis of cooperative mobile cable robots, building upon knowledge base of multi-fingered grasping, and illustrate it with a case study of four cooperating gantry mounted cable robots transporting a planar payload. We show its wrench closure workspace and reconfiguration to extend the workspace, as well as redundancy resolution by optimally repositioning the bases to maximize tension factor along a given trajectory.

1 Introduction

Cable driven parallel manipulators, also called cable-driven robots or cable robots, are formed by attaching multiple cables (instead of articulated links) to an end-effector/platform. They have significantly improved workspace as compared to conventional rigid-link architectures, while possessing many of the desirable features such as high payload-to-weight ratios, low inertial properties, low energy consumption, ease of assembly/disassembly and reconfiguration. Overall low cost and

X. Zhou · V. Krovi
Department of Mechanical and Aerospace Engineering,
State University of New York at Buffalo, Buffalo, NY 14260 USA
e-mail: {xzhou9,vkrovi}@buffalo.edu

C.P. Tang
Caterpillar Global Mining Division, Denison TX 75020 USA
e-mail: nonholonomic@gmail.com

D. Milutinović & J. Rosen (Eds.): Redundancy in Robot Manipulators, LNEE 57, pp. 109–123.
DOI: 10.1007/978-3-642-33971-4_7

reliability contribute to their deployment in many real-world applications, such as heavy payload handling for manufacturing [1], extraterrestrial exploration [2], haptics [3, 4], large scale radio telescopes [5], and load transport [6].

Cooperative payload manipulation using cables comes in two flavors: one class of approaches focuses on fixed bases and varying cable lengths [1, 3, 7, 8] (i.e. conventional cable robots); the other class is with fixed cable lengths and moving bases for manipulating of objects [9] and payload manipulation and transportation on land [10], sea [11], and in the air [12] (i.e. cable towing). In this work, we explore merging the two, i.e. coupling mobile bases with articulated-cable-arms together to create composite mobile-cable collectives for the combined payload transportation and reconfiguration tasks (such as shown in Fig. 1). We call this type of cable robots with moving bases cooperating mobile cable robots. While this combination potentially could greatly increase the capability of cable robots, it also introduces redundancy and complexity into the system. Hence, we will focus on developing a systematic framework for design, analysis and control of such mobile cable robot collectives.

There are many challenges to the development of such a framework. Cable robot systems can function only when the cables are in tension, which creates unilateral constraints on the controlled-input rendering conventional control schemes developed for typical parallel robots incompatible. Workspace determination in the presence of these unilateral constraints creates challenges that will be reviewed in Section 2. Further, despite many parallels exist between the unilateral tension requirements and unidirectional normal-force constraints arising in multi-fingered hands and multi-legged walkers efforts to relate this wealth of literature to cable robots have been very limited [13].

In modularly composed systems, both the nature of the individual modules as well as their interactions can affect the overall system performance. Hence, a systematic (and preferably quantitative) framework for evaluation of the individual

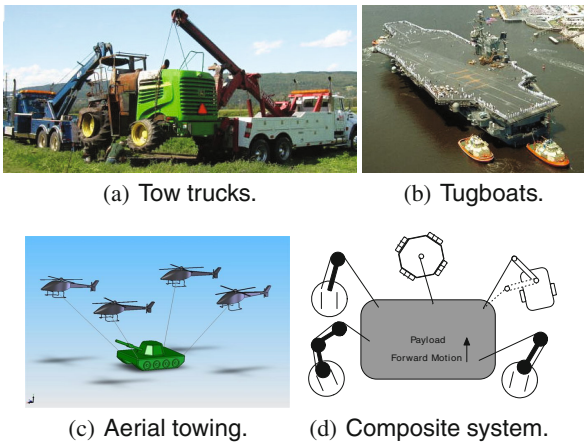

(a) Tow trucks. (b) Tugboats.

(c) Aerial towing. (d) Composite system.

Fig. 1 Illustrative examples of mobile-agent teams tethered to a payload

module- and system-level characteristics is desirable. This is an aspect that we examine in the context of cooperative payload transport by mobile cable robot collectives in this chapter. To this end, we leverage the rich history and background of analysis methods for constrained articulated mechanical systems. In particular, a twist- and wrench-based analysis of in-parallel systems [14, 15] provides the underlying framework for examining the performance of the cooperative system here. *The unique contributions of this chapter come from: (i) the constructive modeling of the individual- and group-capabilities of the cooperating mobile cable robots; (ii) systematic design evaluation of options such as attachment points choices and mobile base positioning; (iii) redundancy resolution by optimal reconfiguration to maximize tension factor along a desired trajectory.*

2 Background

Besides the recent interest in multiple mobile agents, other forms of cooperative multi-robot systems including multi-fingered hands and multi-legged vehicles have been extensively studied in many contexts, as reviewed in [16]. Traditionally, such systems have been modeled as articulated mechanical systems, with the characteristic formation of closed kinematic chains. Apart from the structural classification of Type I (legged) and Type II (multi-arm/multi-finger hand) systems, an alternate functional classification into under-actuated, fully-actuated and redundantly-actuated systems is also possible [16]. It is meaningful to exploit the redundancy in the system to optimize secondary criteria, such as the contact/internal force distribution, in addition to the performance of the motion tasks in multi-legged walkers [17], multi-fingered hands [18] and multi-arm systems [19]. It is important to note that most of these efforts have been addressed in a centralized control context - with the notable exception of [20].

A cable robot with an n DOF end effector requires at least $n+1$ cables to fully constrain the end-effector, leading to minimum limits of four cables for planar robots and seven cables for the spatial case [3]. This also leads to a natural classification into fully-, over- and under-constrained cable-robot systems. In the fully- and over-constrained cable-robot systems, the posture (position/orientation) of the end-effector can be completely determined by the given lengths of the cables and force closure can be achieved [13]. The workspace determination [21, 22, 23, 24] poses challenges - while the potentially-reachable workspace is a function of the geometric configuration (cable lengths, motor mounting position, cable attachment location, etc.), not all postures may be feasible under positive-tension constraints. Hence an additional functional workspace classification becomes possible [24, 7, 25]. In [26], a generic method for determining wrench closure for a fully constrained cable robot is presented. A measure of workspace quality named tension factor is presented in [27], which we will adopt as our optimization criteria. The similarities between cable robots and other parallel architecture manipulators lead to systematic formulation of system performance from individual agent contribution, and we explore this perspective next.

3 Formulation

Using the matrix Lie Group representation of $SE(3)$ based on the notation introduced in [14], let $\{s\}$ and $\{b\}$ be the spatial and body fixed frames, the relative pose of a rigid body may be expressed as $g_{sb} = \left[\begin{smallmatrix} R_{sb} & p_{sb} \\ O & 1 \end{smallmatrix}\right]$, where $R \in SO(3)$ is a rotation matrix and $p \in \mathbb{R}^3$ is a displacement vector. The body twists can be computed as $\underset{\sim}{t}^b_{sb} = g^{-1}_{sb}\dot{g}_{sb}$. The body twist vector corresponding to this twist matrix can be interpreted in terms of linear and angular velocities in body fixed coordinates $\underset{\sim}{t}^b_{sb} = {}^b[v_x, v_y, v_z, \omega_x, \omega_y, \omega_z]^T$. Wrenches $\underset{\sim}{w}^b_{sb} = {}^b[f_x, f_y, f_z, \tau_x, \tau_y, \tau_z]^T$ correspond to co-vector fields and satisfy the virtual work relationship $\underset{\sim}{w} \cdot \underset{\sim}{t} = 0$. The adjoint transformation $Ad_g = \left[\begin{smallmatrix} R & \hat{p}R \\ O & R \end{smallmatrix}\right]$ and the co-adjoint transformation $Ad^T_{g^{-1}} = \left[\begin{smallmatrix} R & O \\ \hat{p}^T R & R \end{smallmatrix}\right]$ serves to transform twists and wrenches between various frames of references.

3.1 Agent Twists

For each cooperating robot (they do not have to be identical), we treat the cable as an articulated prismatic joint extending from its end-effector. Then it is a straight forward process to derive its spatial twist. We can assign the preferred frames and find its body twists of successive joints and then transform to a common frame (for which we choose fixed world frame $\{F\}$ here) to compose the agent's spatial Jacobian $J^s_i(\mathbf{q}_i)$:

$$ {}^F\left[{}^0\underset{\sim}{t}_n\right]_i = J^s_i(\mathbf{q}_i)\dot{\mathbf{q}}_i = \left[{}^F\left[{}^0\underset{\sim}{t}_1\right]_i \ \cdots \ {}^F\left[{}^{n-1}\underset{\sim}{t}_n\right]_i\right], \tag{1} $$

where $\mathbf{q}_i$ are the joint space coordinates. This way, we can incorporate heterogeneous mobile agent collectives (such as shown in Fig. 1(d)) to perform cooperative manipulation.

3.2 Payload Attachment Statics

Since the cables are firmly attached to the payload, there is no slipping. We note that unlike finger pushing, cable pulling does not depend upon object's shape/contact normal direction, rather, it is the cable attachment point's relative position with respect to payload center of mass (COM) that matters. Thus, we define the cable attachment contact frame $\{c_i\}$ to have the same orientation as the payload object COM frame $\{o\}$, as shown in Fig. 2. The transformation from cable attachment frame $\{c_i\}$ to payload frame $\{o\}$ is given by $g_{oc_i} = \begin{bmatrix} R_{oc_i} & p_{oc_i} \\ O & 1 \end{bmatrix}$, where $R_{oc_i} = I$ since we choose attachment frame to have the same orientation as payload object frame, and p_{oc_i}, which are all fixed, once the attachment locations are chosen.

The basis direction of the cable tension in contact frame $\{c_i\}$ is given by B_{c_i}, then the cable wrench can be expressed in the payload object frame $\{o\}$ via co-adjoint

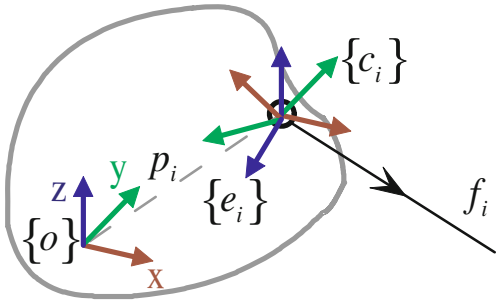

Fig. 2 Cable attachment contact model

transformation as ${}^{o}\underset{\sim}{w}_i = Ad^{T}_{g^{-1}_{oc_i}} B_{c_i} f_i$. Thus, in the payload object frame, the mapping P from the space of the m cable tensions $\mathbf{f}$ to the object wrench $\underset{\sim}{w}_o$ can be expressed as

$$\underset{\sim}{w}_o = P\,\mathbf{f}_{m\times 1} = \begin{bmatrix} | & | & | & | \\ P_1 & P_2 & \cdots & P_m \\ | & | & | & | \end{bmatrix}_{6\times m} \begin{bmatrix} f_1 \\ f_2 \\ \vdots \\ f_m \end{bmatrix}, \tag{2}$$

where $P_i = Ad^{T}_{g^{-1}_{oc_i}} B_{c_i}$. Analogous to the grasp map, we call P the pulling map.

3.3 The Attachment Pulling Constraint

Now that we have both the agent Jacobian and payload attachment statics model, we can write the pulling constraint in terms of relative velocity between attachment contact frame $\{c_i\}$ and cable end frame $\{e_i\}$. The constrained motion direction is the cable pulling direction, which means:

$$B^{T}_{c_i} \underset{\sim}{t}^{b}_{e_i c_i} = 0, \tag{3}$$

where $\underset{\sim}{t}^{b}_{e_i c_i}$ is the body twist between the payload attachment contact frame $\{c_i\}$ and mobile agent cable end frame $\{e_i\}$, expressed in $\{c_i\}$.

Now we seek to rewrite the constraint (3) in known quantities, i.e. we wish to relate payload velocity and agent velocity. We expand $\underset{\sim}{t}^{b}_{e_i c_i}$ as:

$$\underset{\sim}{t}^{b}_{e_i c_i} = Ad_{g_{c_i F}} \underset{\sim}{t}^{b}_{e_i F} + \underset{\sim}{t}^{b}_{F c_i} = -Ad_{g^{-1}_{F c_i}} \underset{\sim}{t}^{s}_{F e_i} + Ad_{g^{-1}_{oc_i}} \underset{\sim}{t}^{b}_{Fo}, \tag{4}$$

where the agent's spatial twist $\underset{\sim}{t}^{s}_{F e_i} = J^{s}_{F e_i} \dot{\mathbf{q}}_i$ as derived earlier, and $\underset{\sim}{t}^{b}_{Fo} = \dot{\mathbf{x}}_o$ is the payload body twist.

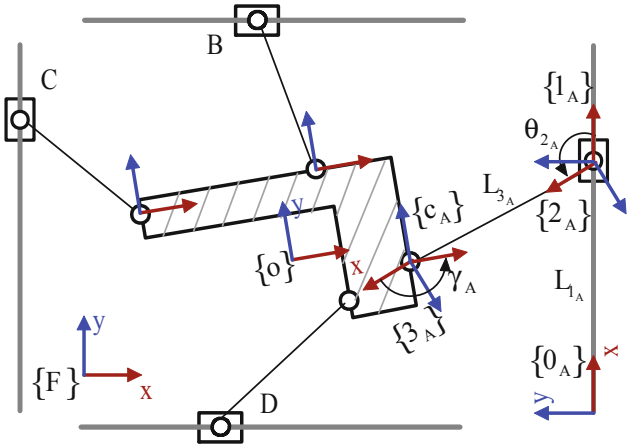

Fig. 3 Payload with 4 Agents (A,B,C,D)

Substituting (4) into (3), we get:

$$J_T(\mathbf{q_T}, \mathbf{x}_o)\dot{\mathbf{q}_T} = P_o^T \dot{\mathbf{x}}_o, \tag{5}$$

where the team Jacobian and the pulling map:

$$J_T = \begin{bmatrix} J_{t1} & & O \\ & \ddots & \\ O & & J_{tm} \end{bmatrix}, \quad P_o^T = \begin{bmatrix} P_1^T \\ \vdots \\ P_m^T \end{bmatrix} = \begin{bmatrix} B_{c_1}^T Ad_{g_{oc_1}}^{-1} \\ \vdots \\ B_{c_m}^T Ad_{g_{oc_m}}^{-1} \end{bmatrix}, \tag{6}$$

where $J_{ti} = B_{c_i}^T Ad_{g_{Fc_i}}^{-1} J_{Fe_i}^s$. We can rewrite the pulling constraint (5) into the form $A_p(q)\dot{q} = 0$, where $A_p = [J_T, \ -P^T]$ and $q = [q_T^T, \ x_o^T]^T$.

4 Planar Gantry Cable Robot Example

As an illustrating example of the process, for simplicity, we consider a planar payload being manipulated by four cooperating gantry-type mobile-crane modules. Each mobile cable robot agent consists of a linear gantry that can translate along one axis with a mounted winch to control the cable length. The distal end of the cable is assumed to be attached to the payload using a pin joint (for simplicity, although a variety of other attachments are possible). Four such mobile cable robot agents are assumed to be attached to a common payload as shown in Fig. 3.

4.1 Formulation

4.1.1 Kinematics

Following the framework presented above, we show how to systematically derive the equations. For this planar case:

$$Ad_g = \begin{bmatrix} R & \begin{bmatrix} p_y \\ -p_x \end{bmatrix} \\ O & 1 \end{bmatrix}, \; Ad^T_{g^{-1}} = \begin{bmatrix} R & 0 \\ -[p_y \;\; -p_x]R & 1 \end{bmatrix}. \tag{7}$$

The joints of each gantry cable agent are $\mathbf{q}_i = [\, l_{1i},\ \theta_{2i},\ l_{3i}\,]^T, \forall i \in \{A,B,C,D\}$. The example reference frames for agent A are shown in Fig. 3, where the $\{3_A\}$ frame is the cable end frame $\{e_A\}$ noted in Section 3. In each successive joint frame, the body twists can be easily found as:

$$\underset{\sim}{t}^b_{01_i} = \begin{bmatrix} \dot{l}_{1_i} \\ 0 \\ 0 \end{bmatrix}, \; \underset{\sim}{t}^b_{12_i} = \begin{bmatrix} 0 \\ 0 \\ \dot{\theta}_{2_i} \end{bmatrix}, \; \underset{\sim}{t}^b_{23_i} = \begin{bmatrix} \dot{l}_{3_i} \\ 0 \\ 0 \end{bmatrix}. \tag{8}$$

Then the spatial Jacobian of each agent can be found as:

$$J^s_{Fei} = \begin{bmatrix} \cos\phi_{0i} & y_{0i} + l_{1i}\sin\phi_{0i} & \cos(\phi_{0i}+\theta_{2i}) \\ \sin\phi_{0i} & -x_{0i} - \cos\phi_{0i} l_{1i} & \sin(\phi_{0i}+\theta_{2i}) \\ 0 & 1 & 0 \end{bmatrix}, \tag{9}$$

where $x_{0i},\ y_{0i},\ \phi_{0i}$ is the position and orientation of the gantry starting frame $\{0_i\}$ in world fixed frame $\{F\}$.

4.1.2 Statics

As shown in Fig. 2, the transformation from cable attachment contact frame $\{c_i\}$ to payload COM frame $\{o\}$ is given by $g_{oc_i} = \begin{bmatrix} I & p_{oc_i} \\ O & 1 \end{bmatrix}$. The basis direction of the cable tension in attachment contact frame $\{c_i\}$ is given by $B_{c_i} = [-\cos\gamma_i,\ \sin\gamma_i,\ 0]^T$, where γ_i is the angle from $\{e_i\}$ to $\{c_i\}$, then the cable wrench can be expressed in the object frame $\{o\}$ via co-adjoint transformation as:

$${}^o\underset{\sim}{w}_i = Ad^T_{g^{-1}_{oc_i}} B_{c_i} f_i = \begin{bmatrix} -\cos\gamma_i \\ \sin\gamma_i \\ y_{oc_i}\cos\gamma_i + x_{oc_i}\sin\gamma_i \end{bmatrix} f_i \,. \tag{10}$$

We can concatenate the four cable wrenches into:

$$\begin{bmatrix} F_x \\ F_y \\ M_z \end{bmatrix} = \begin{bmatrix} | & | & | & | \\ P_A & P_B & P_C & P_D \\ | & | & | & | \end{bmatrix} \begin{bmatrix} f_A \\ f_B \\ f_C \\ f_D \end{bmatrix}, \tag{11}$$

where $P_i = Ad^T_{g_{oc_i}^{-1}} B_{c_i}$, $\forall i = A, \ldots, D$. This is the pulling map (2) that maps the cable tension forces $\mathbf{f}$ to the object wrench $\underset{\sim}{w}_o$ in the payload frame.

4.1.3 Pulling Constraint

The velocity level constraints can be developed by projecting the relative velocity difference of the cable tip and the payload along the line of action of the cable (which is the pulling direction). This relative velocity is now expected to be equal to zero in order to avoid cable slack.

As derived in Section 3.3, for the pulling constraint (5) in body frame, we have:

$$P_{oi} = \begin{bmatrix} -\cos(\phi_o - \phi_{0i} - \theta_{2i}) \\ \sin(\phi_o - \phi_{0i} - \theta_{2i}) \\ y_{c_i}\cos(\phi_o - \phi_{0i} - \theta_{2i}) + x_{c_i}\sin(\phi_o - \phi_{0i} - \theta_{2i}) \end{bmatrix}, \tag{12}$$

and the team Jacobian is:

$$J_T = \begin{bmatrix} J_{t1} & & O \\ & \ddots & \\ O & & J_{tm} \end{bmatrix}, \tag{13}$$

where $J_{ti} = [-\cos\theta_{2_i},\ \cos(\phi_{0_i} + \theta_{2_i})y_o + \sin(\phi_{0_i} + \theta_{2_i})(x_{0_i} + \cos\phi_{0_i} l_{1_i}) - \cos(\phi_{0_i} + \theta_{2_i})(y_{0_i} + l_{1_i}\sin\phi_{0_i}) - \sin(\phi_{0_i} + \theta_{2_i})x_o + y_{c_i}\cos(\phi_o - \phi_{0_i} - \theta_{2_i}) + x_{c_i}\sin(\phi_o - \phi_{0_i} - \theta_{2_i}),\ -1]$.

4.2 Case Study 1: Wrench Closure Workspace and Its Quality

We now consider the ability of the system to both generate and resist arbitrary payload wrenches (i.e. wrench closure). We use the simple planar example of an "L" shaped payload manipulated by four gantry cable robots to showcase the benefits of the systematic formulation. In particular, we will focus attention on using quantitative metrics derived from this formulation to determine the wrench closure workspace and its quality.

4.2.1 Wrench Closure Condition

For planar cases, it is possible to analytically determine the workspace such as shown in [24]. Considering applicability to spatial cases, the numerical algorithm presented in [26] can be used to determine wrench closure for general $m > n$ cases and it is relatively fast in computation. It basically says a necessary and sufficient condition for wrench closure is a test vector such as $p_t = -\sum_{i=1}^{n} p_i$ can be positively

spanned by another set of basis of the pulling map P. The algorithm itself is straight forward, whose details can be found in [26].

We show a sample calculation of the workspace when the gantries are positioned in the middle of their stroke and the attachment points are at the four tips of the payload. We check for wrench closure condition across the workspace with the payload orientation angle ϕ varying from -40 to 40 degrees. Fig. 4 shows the resulting workspace.

4.2.2 Workspace Quality

Apart from simple wrench closure, it would be useful to know the quality of the workspace. One measure is the tension factor(TF) as defined in [27]:

$$TF = \frac{min(\mathbf{f})}{max(\mathbf{f})}. \tag{14}$$

Since cable tensions are positive, then $0 < TF \leq 1$. A larger TF means a more even distribution of tensions in cables. It is shown that maximizing TF is equivalent to the following linear optimization problem:

$$\begin{aligned} \text{minimize} \quad & \sum_{i=1}^{m} f_i \\ \text{subject to} \quad & P\mathbf{f} = 0 \\ & f_i \geq f_{i_{min}} > 0, \quad (i = 1, 2, \ldots, m) \end{aligned} \tag{15}$$

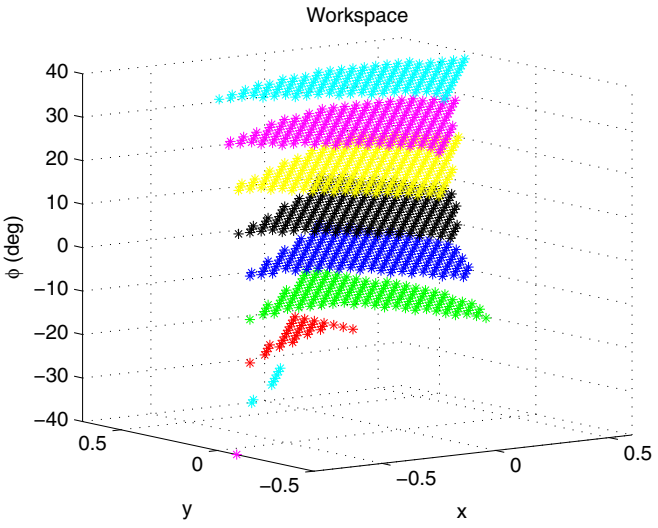

Fig. 4 Wrench closure workspace

Figure 5 shows the quality of the workspace when the gantries are positioned in the middle of their stroke and the attachment points are at the four tips of the payload. The tension factors are represented by the relative size of the square markers. We can see that due to the asymmetric payload shape, the workspace is irregular and its quality in the sense of tension factors is even more limited. The high redundancy in the base positioning allows us to optimize the design.

4.3 Case Study 2: Design Optimization

We first show a simple illustration of the idea. As can be easily seen, Fig. 6(a) is not wrench closure. Intuitively, we have two design choices to make it wrench closure: one is by changing attachment point location (as shown in Fig. 6(b)); and the other is by moving the base location (as shown in Fig. 6(c)). While this is simply done by inspection, in general, the selection of cable attachment point position/base location for asymmetric payloads tends to be non-intuitive.

Next we perform design optimization based on our systematic formulation to the example. The "L" shaped payload is assumed to be general with non uniform mass density and thus its COM does not coincide with its geometric area center. It is in circumstances such as this that the systematic formulation coupled with quantitative analysis can be very useful for design and analysis.

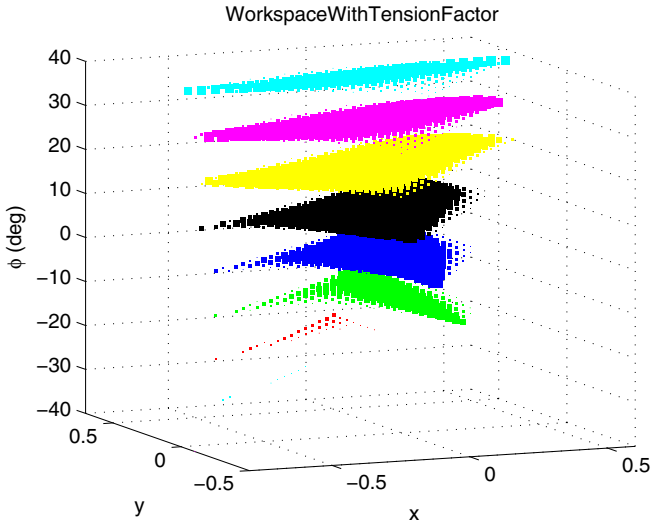

Fig. 5 Workspace tension factor (size of the cubes proportional to TF value)

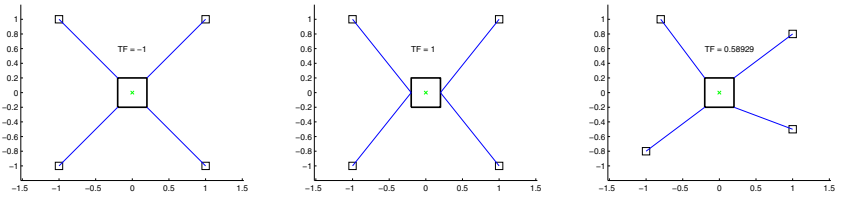

(a) Non closure. (b) Move attachment. (c) Move base.

Fig. 6 Simple illustration of reconfiguration

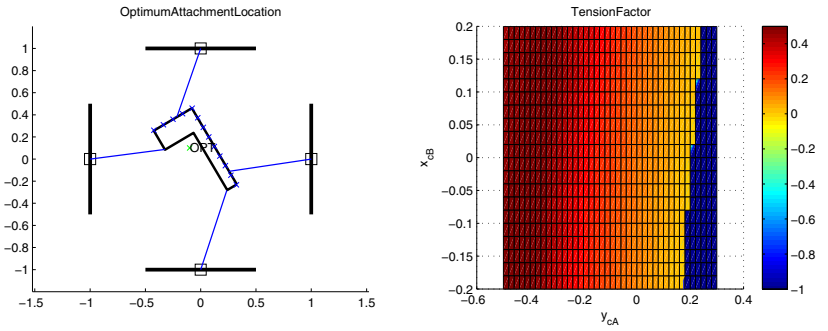

(a) Optimal attachment. (b) TF vs attachment.

Fig. 7 Effect of cable attachment choice

4.3.1 Cable Attachment Choices

We first consider optimizing the cable attachment point locations on the payload. The gantries are fixed at the center of their stroke, which essentially reduces our model to the conventional fixed-base cable robot case.

The base gantries are immobilized at the mid point ($l_{1_i} = 0.5,\ \forall i = A,\ \ldots,\ D$) of their full stroke. The payload COM is at $x_o = -0.1,\ y_o = 0.1, \phi_o = 30^\circ$. We perform a parametric sweep to study the role of cable attachment positioning to payload on the wrench closure condition of the pulling map, as shown in Fig. 7. Two of the cable attachment points on the payload are held fixed at the tips while the other two attachments can be repositioned anywhere along the corresponding sides (y_{c_A} and x_{c_B}).

The tension factors for each configuration is shown in Fig. 7(b). We set the tension factor to -1 to clearly represent wrench singular (not wrench closure) configuration. The attachment locations corresponding to optimal tension factor is shown in Fig. 7(a).

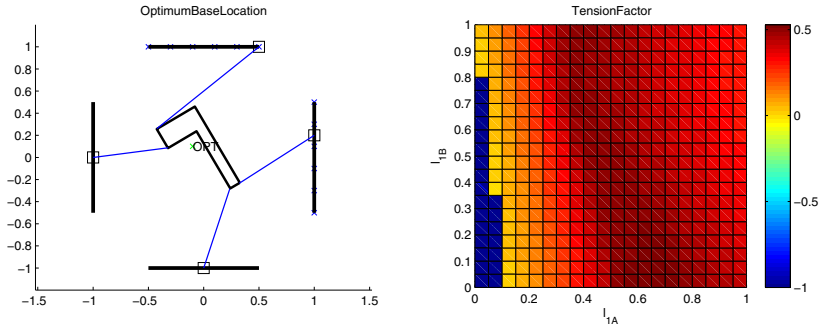

(a) Optimal base. (b) TF vs base.

Fig. 8 Effect of base repositioning

4.3.2 Choices of Mobile Bases

It may be relatively inconvenient to change attachment points on the fly (i.e. re-grasping); reconfiguring the mobile bases is more useful in practical situations. Again, we perform a parametric sweep to study the role of base positioning on the wrench closure of the pulling map. The cable attachment points on the payload are held fixed at the four corner. Two of the base gantries are immobilized at the mid point ($l_{1_C} = 0.5$, $l_{1_D} = 0.5$) of their full stroke, while the other two base gantries can be repositioned anywhere along their full stroke (l_{1_A} and l_{1_B}).

Fig. 8(b) showcases the tension factor plotted against the gantry positions (l_{1_A} and l_{1_B}). As a result, the pose that has the largest tension factor is shown in Fig. 8(a). While the above results were shown in the form of parametric sweep results for two design variables at a time, this was done solely for visual illustration. Various optimization methods can now be systematically applied to a full fledged multi-variable case which is shown next.

4.4 Case Study 3: Maintaining Optimal Tension Factor Along Trajectory

In addition to the previous "static" design optimization of either attachment location or base position, a more useful way would be to "dynamically" resolve the redundancy by optimally reconfiguring the base gantry location along a desired trajectory (such as the case in Fig. 9). This way, tension factor can be maintained the highest possible all the time. This problem can be solved using "cascaded" optimization. Basically we wrap an optimization of the four gantry positions on top of the optimization of tension factor.

Different from conventional parallel robot singularities, there is no analytical solution to wrench closure. Therefore conventional singularity avoidance techniques using redundancy to optimize the smallest singular value are infeasible for the mobile cable robots here. There is no analytical gradient, and numerical approximation

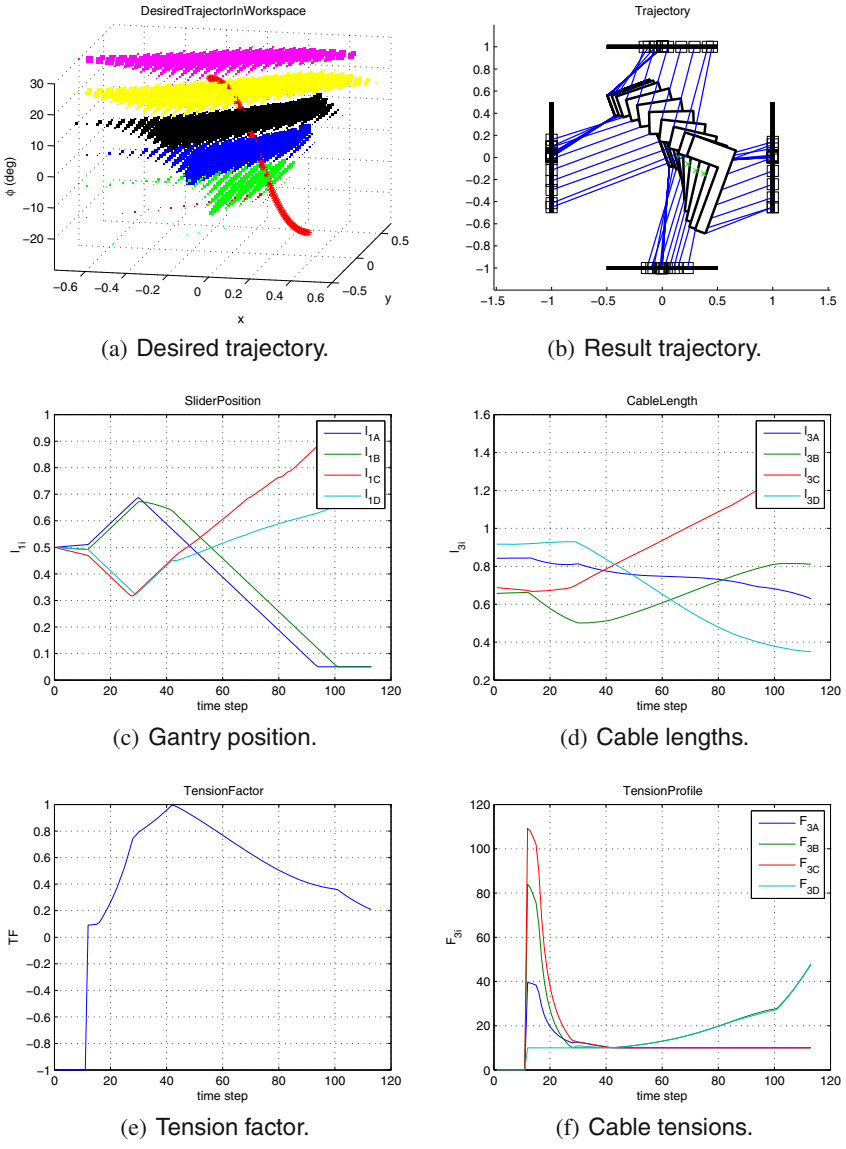

(a) Desired trajectory. (b) Result trajectory.

(c) Gantry position. (d) Cable lengths.

(e) Tension factor. (f) Cable tensions.

Fig. 9 Reconfiguration to optimize tension factor along trajectory

is not a good solution due to high nonlinearity of the pulling map with respect to configuration change. Either a pre-calculation/planning of trajectories to avoid singularity (which is computationally expensive) or reconfiguration along the way is needed.

In case of wrench singular (not wrench closure) configurations of the mobile cable robots during the trajectory, two simple approaches can be used to resolve it: one

is to perform a global optimization to find a feasible bases configuration, then interpolate in the internal joint space to reach the feasible configuration and initialize from there; the other is to perform a local search by exploratory moves of the mobile bases which should be faster and possible if it is not far off. Also this might lead to a local optimal tension factor, but it is acceptable in the case of trajectory tracking. To ensure continuity, we also impose maximum velocity of gantry as an additional constraint to be practical, otherwise optimization results may drive the gantries all over the place and thus causing discontinuity just to get the best tension factor. Higher order of continuity can be achieved by imposing acceleration/jerk level constraints to get a smoother result.

We note here in our case with only one redundant cable, the null space of the pulling map has only one dimension. So the wrench closure condition in [26] and tension factor in [27] can be simplified. It is straight forward to show wrench closure is equivalent to requiring components of the null space vector to have same sign, and tension factor is equivalent to the ratio of minimum and maximum of the absolute values of the null space vector. This way, the lower level optimization is reduced and thus saving us some computation time.

Here we show an example of transporting the payload along a desired trajectory as shown in Fig. 9(a). The starting point is out of the wrench closure workspace for the initial base configuration, which is also evident in Fig. 9(e), as the starting tension factor is -1 indicating non wrench closure. It can be seen from Fig. 9(b), after a few exploratory steps, the gantry bases move to a feasible configuration, and then afterwards the redundant gantry positions are optimized (using MATLAB Optimization Toolbox) to maintain a configuration that yields the best possible tension factor as shown in Fig. 9(e). We note that instead of performing optimization, planning algorithms such as RRT may also be used for reaching an initial feasible configuration. The resulting gantry position is shown in Fig. 9(c), cable length profile in Fig. 9(d), and corresponding positive cable tensions in Fig. 9(f). We also note that with high reconfigurability of mobile bases, wrench closure condition can actually be relaxed (i.e. three mobile cable robots transporting payload) if it is not required to exert/resist arbitrary wrench, as along as the configuration is able to exert certain required dynamics forces/moments along a given trajectory. This aspect is currently being pursued.

5 Discussion

The addition of base mobility provides cable robots greater flexibility, yet it requires careful investigation. In this chapter we extend a systematic screw theoretic formulation approach to the general cooperating cable robots on mobile bases. In particular, creating a formalism for studying system level configuration by composing the contributions of individual agents and thereby creating a parametric model is attractive. Various parametric analysis including parameter sweeps, optimization and sensitivity analysis, can now be brought to aid design and analysis. Another benefit is the ready extensibility of framework to full fledged spatial cases using this formalism. Using this formulation also permits close linkage between grasping, walking and

in general parallel robots, allowing for cross-pollination of results. Physical system validation for cooperative ground mobile robots is currently underway.

References

1. Albus, J., Bostelman, R., Dagalakis, N.: Journal of Robotic Systems 10(5), 709 (1993)
2. Huntsberger, T., Stroupe, A., Aghazarian, H., Garrett, M., Younse, P., Powell, M.: Journal of Field Robotics 24(11), 1015 (2007)
3. Kawamura, S., Ito, K.: Proceedings of the IEEE/RSJ International Conference on Intelligent Robots and Systems, Yokohama, Japan (1993)
4. Williams II, R.L.: International Journal of Virtual Reality 3(3), 13 (1998)
5. Nan, R.: Science in China Series G: Physics Mechanics and Astronomy 49(2), 129 (2006), doi:10.1007/s11433-006-0129-9
6. Oh, S.R., Ryu, J.C., Agrawal, S.K.: ASME Journal of Mechanical Design 128(5), 1113 (2006)
7. Fattah, A., Agrawal, S.K.: ASME Journal of Mechanical Design 127(5), 1021 (2005)
8. Meunier, G., Boulet, B., Nahon, M.: IEEE Transactions on Control Systems Technology 17(5), 1043 (2009)
9. Donald, B., Gariepy, L., Rus, D.: Proceedings of IEEE International Conference on Robotics and Automation, ICRA 2000, vol. 1, pp. 450–457 (2000)
10. Cheng, P., Fink, J., Kumar, V., Pang, J.S.: ASME Journal of Mechanisms and Robotics 1(1), 1 (2009)
11. Esposito, J., Feemster, M., Smith, E.: IEEE International Conference on Robotics and Automation, ICRA 2008, pp. 1501–1506 (2008)
12. Michael, N., Fink, J., Kumar, V.: Robotics: Science and Systems V (2009)
13. Voglewede, P.A., Ebert-Uphoff, I.: IEEE Transactions on Robotics 21(4), 713 (2005)
14. Murray, R.M., Li, Z., Sastry, S.S.: A Mathematical Introduction to Robotic Manipulation. CRC Press, Boca Raton (1994)
15. Waldron, K.J., Hunt, K.H.: The International Journal of Robotics Research 10(5), 473 (1991), http://ijr.sagepub.com/content/10/5/473.abstract, doi:10.1177/027836499101000503
16. Tang, C.P., Krovi, V.: Robotica 25(1), 29 (2007)
17. Kumar, V., Waldron, K.J.: ASME Journal of Mechanisms, Transmissions, and Automation in Design 112(1), 90 (1990)
18. Salisbury, J.K., Roth, B.: ASME Journal of Mechanisms, Transmissions and Automation in Design 105(1), 35 (1983)
19. Paljug, E., Yun, X., Kumar, V.: IEEE Transactions on Robotics and Automation 10(4), 441 (1994)
20. Liu, Y.H., Arimoto, S.: IEEE Transactions on Automatic Control 41(8), 1193 (1996)
21. Bosscher, P., Riechel, A.T., Ebert-Uphoff, I.: IEEE Transactions on Robotics 22(5), 890 (2006)
22. Ghasemi, A., Eghtesad, M., Farid, M.: ASME Journal of Mechanisms and Robotics 1(4), 044502 (2009)
23. Stump, E., Kumar, V.: ASME Journal of Mechanical Design 128(1), 159 (2006)
24. Gouttefarde, M., Gosselin, C.M.: IEEE Transactions on Robotics 22(3), 434 (2006)
25. Barrette, G., Gosselin, C.M.: Journal of Mechanical Design 127(2), 242 (2005)
26. Lim, W.B., Yang, G., Yeo, S.H., Mustafa, S.K., Chen, I.M.: IEEE International Conference on Robotics and Automation, ICRA 2009, pp. 2187–2192 (2009)
27. Pham, C.B., Yeo, S.H., Yang, G., Chen, I.M.: Robotics and Autonomous Systems 57(9), 901 (2009)